

Geophysical Research Letters

RESEARCH LETTER

10.1029/2019GL083395

Key Points:

- Statistical data assimilation is used to retroactively forecast the 2008 eruption of Okmok volcano, Alaska, which lacked clear precursors
- Numerical models track the evolving stress state of the Okmok magma system and forecast eruption likelihood at each time step
- Model forecasts indicate that the system was trending toward tensile failure in the weeks leading up to the 2008 eruption

Supporting Information:

- Supporting Information S1

Correspondence to:

J. A. Albright,
johnaa2@illinois.edu

Citation:

Albright, J. A., Gregg, P. M., Lu, Z., & Freymueller, J. T. (2019). Hindcasting magma reservoir stability preceding the 2008 eruption of Okmok, Alaska. *Geophysical Research Letters*, *46*.
<https://doi.org/10.1029/2019GL083395>

Received 18 APR 2019

Accepted 17 JUL 2019

Accepted article online 25 JUL 2019

Hindcasting Magma Reservoir Stability Preceding the 2008 Eruption of Okmok, Alaska

J. A. Albright¹ , P. M. Gregg¹ , Z. Lu² , and J. T. Freymueller³ 

¹Department of Geology, University of Illinois at Urbana-Champaign, Champaign, IL, USA, ²Huffington Department of Earth Sciences, Southern Methodist University, Dallas, TX, USA, ³Department of Earth and Environmental Sciences, Michigan State University, Lansing, MI, USA

Abstract Volcanic eruptions pose a significant and sometimes unpredictable hazard, especially at systems that display little to no precursory signals. For example, the 2008 eruption of Okmok volcano in Alaska notably lacked observable short-term precursors despite years of low-level unrest. This unpredictability highlights that direct monitoring alone is not always enough to reliably forecast eruptions. In this study, we use the Ensemble Kalman Filter (EnKF) to produce a successful hindcast of the Okmok magma system in the lead up to its 2008 eruption. By assimilating geodetic observations of ground deformation, finite element models track the evolving stress state of the magma system and evaluate its stability using mechanical failure criteria. The hindcast successfully indicates an increased eruption likelihood due to tensile failure weeks in advance of the 2008 eruption. The effectiveness of this hindcast illustrates that EnKF-based forecasting methods may provide critical information on eruption probability in systems lacking obvious precursors.

Plain Language Summary Volcano monitoring agencies routinely use increases in volcanic unrest as indicators of the potential for eruption. However, for some eruptions, such as the 2008 eruption of Okmok volcano in Alaska, these behaviors can be subtle or missing altogether. In this study, a new statistics-based volcano forecasting approach is used to test whether computer models are able to capture an increase in eruption likelihood leading up to the 2008 event. The models indicate that Okmok was trending toward eruption weeks in advance due to the increased probability of failure of the magma chamber. This successful test indicates that stress around the magma chamber is a strong predictor of volcano stability and that this method could apply to active volcanic systems and improve hazard mitigation efforts.

1. Introduction

The ability to forecast volcanic eruptions has long been a goal for monitoring agencies and the broader scientific community, with the potential to be a powerful tool in mitigating the risks posed by restless volcanoes to human life, property, and activity. Ground deformation in response to magmatic processes has been the focus of much research in this regard (Segall, 2013; Sparks, 2003; Voight et al., 1998) and played a critical role in informing the successful forecast of Axial Seamount's 2015 eruption (Nooner & Chadwick, 2016). Although more general studies of subaerial volcanoes have found a broad correlation between deformation and the timing of eruptions, their relationship is more complex than at Axial Seamount and provides no clear criteria for eruption based on the magnitude or rate of deformation alone (Biggs et al., 2014; Biggs & Pritchard, 2017). In this study, we seek to further explore this relationship by focusing on the mechanical stress state around the magma reservoir, which is both reflected in the surface deformation and ultimately determines when and how the host rock fractures, opening conduits for magma ascent and eruption.

The Ensemble Kalman Filter (EnKF) is a statistical data assimilation technique (Evensen, 1994, 2003, 2009a, 2009b) that improves on earlier formulations of the Kalman Filter, many of which have already been successfully applied to geodetic data (Aoki et al., 1999; Fournier et al., 2009; McGuire & Segall, 2003; Miyazaki et al., 2004; Segall & Matthews, 1997). Previous studies in other fields of earth science have demonstrated the EnKF's ability to combine large and/or varied data sets with sophisticated models of nonlinear processes (Allen et al., 2003; Brusdal et al., 2003; Natvik & Evensen, 2003; Seiler et al., 2009; Wilson et al., 2014), making it particularly well suited for studying active, monitored volcanoes. Following a framework developed by previous studies (Bato et al., 2017; Gregg & Pettijohn, 2016; Zhan & Gregg, 2017), the EnKF is applied to the 2008 eruption of Okmok volcano, Alaska, to produce a retroactive forecast, or "hindcast,"

of magma system stability. The resulting investigation highlights the importance of tracking volcano stress evolution to forecast eruption potential at active systems.

2. The 2008 Eruption of Okmok Volcano, Alaska

Although Okmok has hosted large explosive eruptions in the past, including a caldera-forming event at ~ 2.4 ka (Miller & Smith, 1987), recorded eruptions since 1945 have been dominated by effusive flows emanating from Cone A on the western side of the caldera, with only modest ash columns present (Beget et al., 2005). After its 1997 eruption, Okmok became the target of multiple research efforts including synthetic aperture *radar* (SAR) satellite analyses, yearly GPS campaigns (2000–2005), and the installation of 12 permanent seismometers and 4 continuous GPS stations in 2003 (Figure 1). Continuous inflation was observed starting from the first posteruption observations in 1997, with episodic pulses of more rapid inflation in the late 1990s, 2002–2003, and 2004–2005, each lasting several months (Fournier et al., 2009; Lu et al., 2010). Geodetic data captured deformation commencing again in early 2008, after 3 years of quiescence and/or slight deflation (Lu et al., 2010). After the failure of the two GPS sites within the caldera in March 2008, interferometric synthetic aperture *radar* (InSAR) data continued to show inflation until the sudden onset of eruption on July 12 (Figure 2).

Unlike the 1997 eruption, the 2008 event formed a new vent near Cone D on the eastern side of Okmok caldera (Larsen et al., 2009). Due to phreatomagmatic interactions between fresh magma and the local water table, the explosive eruption reached VEI 4 and produced a 16-km high ash column (Larsen et al., 2009). Despite the magnitude of the eruption, it lacked a clear precursory signal in its ground deformation. Furthermore, seismic activity had been quiet in the preceding months until a 3- to 5-hr long, low-magnitude precursory earthquake swarm was recorded 11 hr prior to the 2008 eruption (Larsen et al., 2009).

3. Geodetic Data Assimilation to Provide Model Forecasts

The EnKF is utilized to combine geodetic observations of surface deformation at Okmok with finite element models (FEM) of the evolving Okmok magma system. Specifically, GPS and InSAR data are assimilated into a two-dimensional, axisymmetric, linear elastic FEM. In this implementation, the EnKF analysis consists of 300 models, which are updated sequentially in parallel as observations become available from GPS and/or InSAR. The EnKF tracks the observed deformation, providing a good fit to the geodetic data (Figure 2). Although there is slight misfit due to the assumed symmetry of the model, the modeled pressure source is in relative agreement with previous static inversions (Biggs et al., 2010; Fournier et al., 2009; Lu et al., 2005, 2010). Although petrologic and geochemical findings suggest a more complex reservoir geometry, with several distinct shallow reservoirs fed by a deeper source (Larsen et al., 2013), the geodetic data considered here and in previous studies are sufficiently accounted for by a single-source model and lack clearly distinct signals from both a shallow and a deep reservoir.

Overall, a joint GPS + InSAR assimilation approach works best for Okmok. In particular, InSAR provides critical spatial coverage between GPS stations, while continuous GPS signals provide important model updates during temporal gaps in InSAR data collection. Additional EnKF experiments were conducted to investigate the assimilation of GPS or InSAR data alone and are provided in the supporting information. However, the single-technique assimilation approaches both failed to successfully hindcast the 2008 eruption, indicating that the combination of spatial and temporal data coverage is necessary. In particular, the GPS-only assimilation underestimates the depth of the reservoir relative to the joint assimilation and overestimates its lateral extent and aspect ratio (Figure S10), thus predicting failure prematurely (Figure S11). The loss of data from two malfunctioning stations within the caldera most likely contributed to this poor performance as well, since the absence of such proximal stations can significantly reduce the accuracy of the EnKF (Zhan & Gregg, 2017). In contrast to the GPS results, the pressure source modeled by the InSAR-only assimilation overestimates the stability of the reservoir and fails to forecast any eruption-producing failure in 2008 (Figure S14).

4. The Evolving State of Okmok's Magma System

An advantage of the EnKF approach is that model parameters are updated at each time step of the assimilation, allowing for the evolution of the magma reservoir to be evaluated (Figure 3). Additionally, the observed

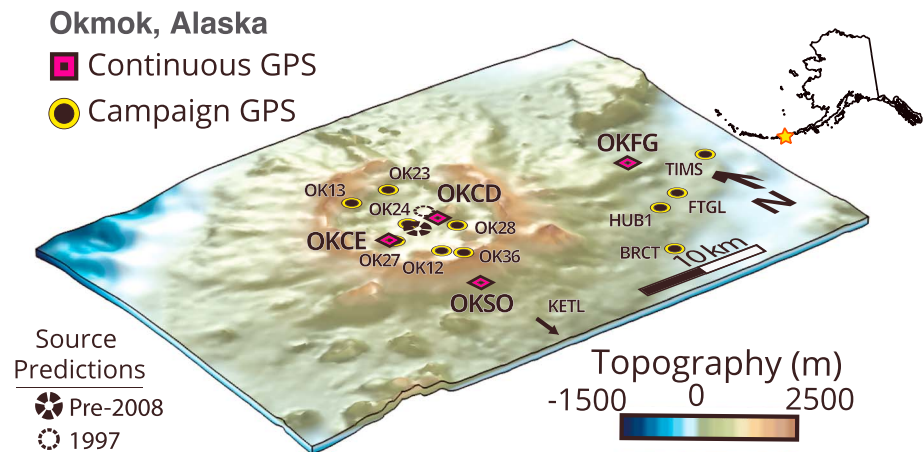


Figure 1. Three-dimensional perspective map of Okmok Volcano, Alaska, showing topography and locations of GPS stations used in this study. Black markers compare the center of preruptive inflation calculated in this study with the coeruptive deflation center found for the 1997 eruption (Mann et al., 2002). Cone A lies south of OKCE, while Cone D lies slightly east of station OKCD.

spread of the parameter values within the ensemble provides a first-order estimate of uncertainty in each parameter (Evensen, 2009a). We assimilated data from 2003 to 2008, starting with the first SAR image of our data set on 10 June 2003. Uncertainty is high during the first year of the assimilation due to the volcano being in a period of quiescence with little deformation. However, all of the parameters quickly converge in 2004, coinciding with the first observed period of major inflation.

The resultant pressure source location agrees with previous studies, which estimate a stationary source located ~3 km beneath the center of Okmok's caldera (Biggs et al., 2010; Fournier et al., 2009; Lu et al.,

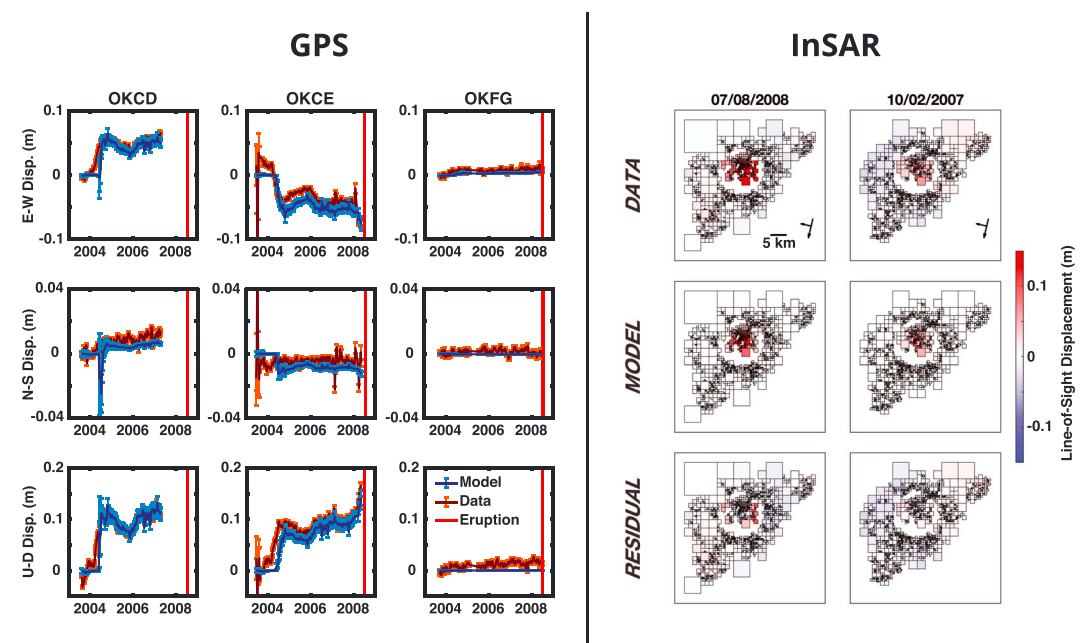


Figure 2. Comparison of deformation predicted by the Ensemble Kalman Filter (EnKF) assimilation results with original data from selected GPS stations and interferometric synthetic aperture radar (InSAR) images. GPS data have been averaged into 10-day bins, while the cumulative InSAR data have been downsampled via a quadtrees algorithm and averaged within the boxes pictured. The EnKF approach sequentially assimilates both GPS and InSAR data as they become available. Comparisons with all available data and additional model runs with GPS only and InSAR only calculations are available in the supporting information.

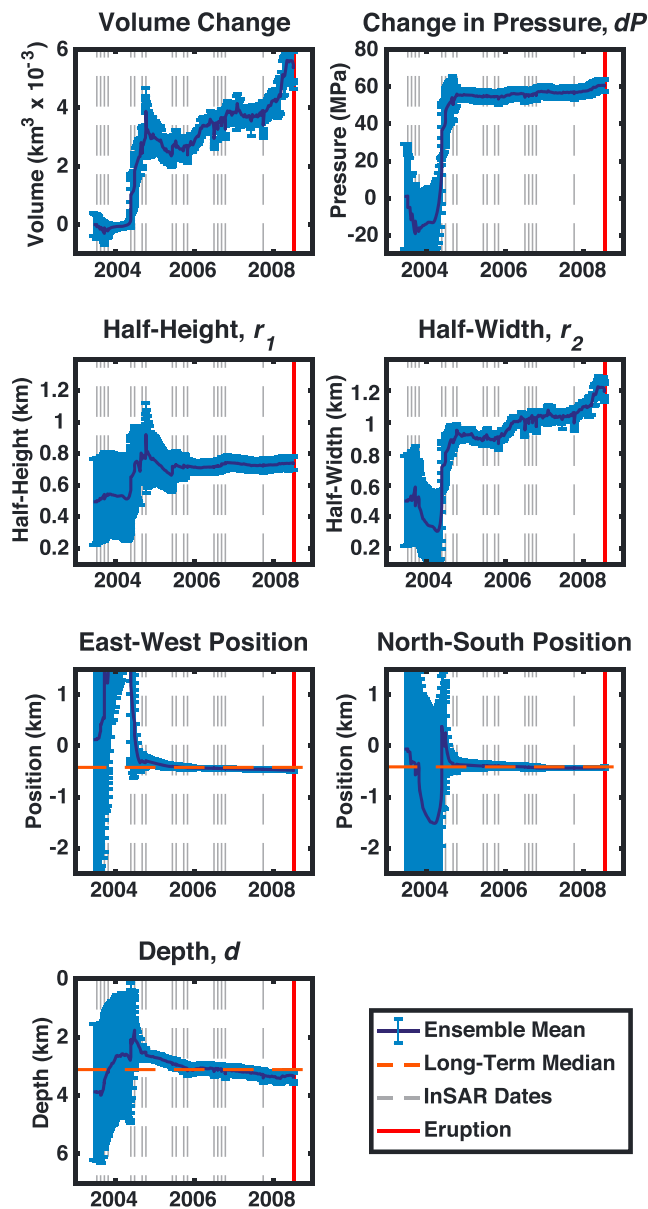


Figure 3. Ensemble Kalman Filter predictions for the six variables modeled in this study, as well as an aggregate volume change term derived from the other values. Uncertainty at each time step is given by twice the observed standard deviation in each parameter across the ensemble ($N = 300$). InSAR = interferometric *synthetic* aperture radar.

2005, 2010). To characterize the magma reservoir, our model assumes an ellipsoidal shape and separately tracks the half height, half width, and pressure change, which are then combined into a single volume change term according to the bulk modulus of the host rock. Pressure increases ~ 60 MPa during the 2004–2005 inflation event but then remains mostly stable throughout the rest of the assimilation, with only slight increases during the second period of inflation in 2008. Similarly, the reservoir half height remains somewhat constant through 2008, leaving an increasing half width as the primary driver of inflation. The model result of lateral reservoir growth, rather than changing pressure, has significant implications for our understanding of the evolution of the magma system in the lead up to the eruption.

Previous studies of GPS deformation at Okmok observed nonzero circumferential motion prior to the eruption (Fournier et al., 2009; Freymueller & Kaufman, 2010). This phenomenon requires changes in the source geometry and cannot be reproduced through increases in pressure alone. The observed shift in the main eruption vent from Cone A to Cone D may also imply a change in the geometry of the magma system more generally, but our models do not make any specific predictions as to how magma reaches the surface once the reservoir has mechanically failed.

5. Linking Model Forecasts to Eruption Triggers

At each time step throughout the assimilation, we track three potential catalysts for eruption: overpressure, Mohr-Coulomb failure, and tensile rupture. The excess pressure within the reservoir quickly exceeds 10–40 MPa (often cited as a limit for initiating and propagating a dike to the surface; e.g., Rubin, 1995) by late 2004 and then remained effectively constant leading up to the eruption. These findings suggest that a critical overpressure alone was not sufficient to trigger the 2008 eruption. Within a region surrounding and overlying the magma reservoir we also tested for Mohr-Coulomb failure. Although the majority of models in the ensemble showed some degree of failure throughout the assimilation, the effect was always localized near the surface of the model space and never resembled the through-going failure suggested as an eruption trigger by other studies (Cabaniss et al., 2018; Gregg et al., 2012; Gregg et al., 2018). Finally, we define tensile rupture of the reservoir to occur when the least compressive stress exceeds the rock’s tensile strength at some point along the reservoir wall (Grosfils, 2007).

The percentage of ensemble members in tensile failure is used as an aggregate and relative measure of reservoir stability throughout the assimilation (Figure 4a). Unlike overpressure and Mohr-Coulomb failure, which tend to vary little over the observed time period, the abundance of tensile

failure strongly correlates with the behavior of the system, displaying two peaks in 2005 and 2008 during or shortly after the periods of greatest inflation. The tensile strength assumed for the wall rock also plays a significant role in determining the system’s stability. When a strength of 0 MPa is assumed, approximating a case in which preexisting fractures have compromised the rock’s cohesion, failure is present in $\sim 20\%$ more ensemble members than when a tensile strength of 10 MPa is used. However, regardless of the strength assumed, the entire ensemble trends toward higher tensile stresses and by extension likelihood of failure throughout 2008 (Figure 4b). This tensile rupture occurs predominantly along the reservoir’s outer rim, which lies in close proximity to the eruption vent near Cone D (Figure 4c). Moreover, the fact that this spike occurs within months of the actual onset of eruption suggests that our assimilation framework is able to reliably account for the accumulation of stress around the magma reservoir through the preceding years,

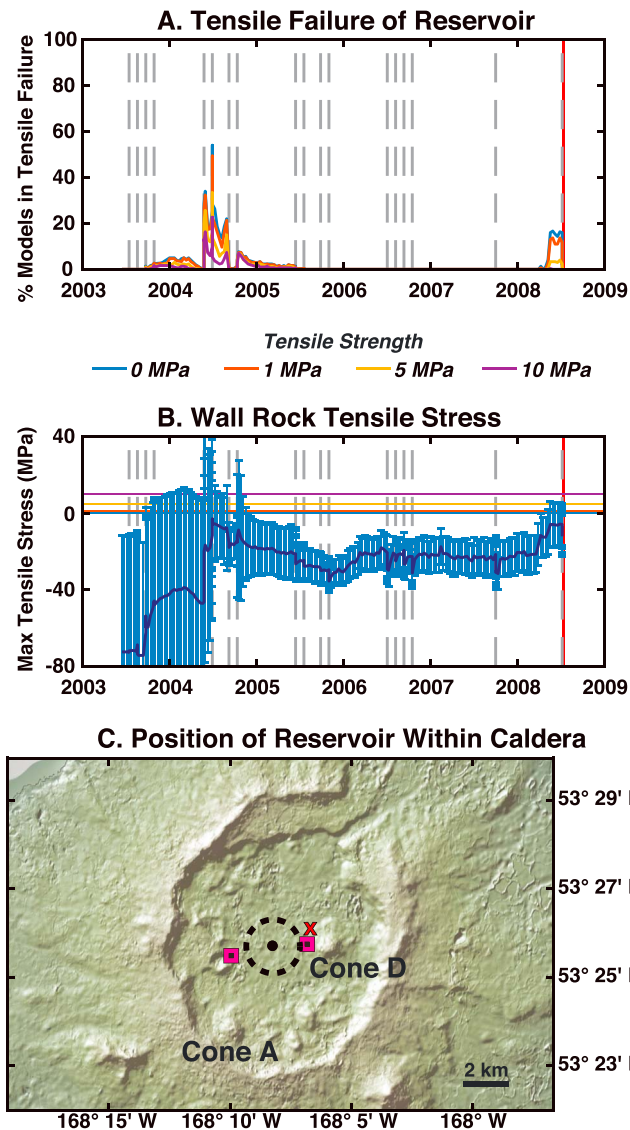


Figure 4. The evolution of predicted tensile failure in the lead up to the 2008 eruption. (a) Percentage of ensemble members exceeding tensile failure criterion at each time step for four different tensile strengths. An ensemble member is considered to be in failure if tensile stress exceeds the given tensile strength at any point along the reservoir wall. (b) Maximum tensile stress calculated along the reservoir wall by Ensemble Kalman Filter assimilation at each time step. Solid line indicates ensemble mean with 2σ error bars. Horizontal lines indicate threshold tensile strengths. (c) Map view of Okmok Caldera showing the center (dot) and extent (dotted line) of the forecasted reservoir (black) relative to nearby continuous GPS stations (purple squares), intracaldera cones, and the primary vent of the 2008 eruption (red X).

producing a successful hindcast of the 2008 event. Such information may have allowed the Alaska Volcano Observatory (AVO) to raise the alert level at Okmok and increase monitoring efforts, potentially catching the preeruptive seismicity as well as the eruption itself.

An alternative triggering mechanism not directly modeled in this study due to technical limitations is the progressive weakening of the host rock during preeruptive deformation. Previous studies at other systems (e.g., Got et al., 2017), have shown that fracturing and seismicity in the edifice above the reservoir can produce a significant weakening in the rock's mechanical properties. However, given the scant and low-intensity nature of the preeruptive seismic signal at Okmok (Larsen et al., 2009) and the lack of fault-related deformation in the geodetic data, it is unlikely that enough fracturing occurred in the months before the eruption to significantly impact its onset. Such a lack of fracturing would also agree with our assimilation's prediction of very little Mohr-Coulomb failure.

6. Implications for Eruption Forecasting at Volcanic Systems

Our results show that the EnKF is a powerful tool for combining multiple streams of observational data with complex numerical models to provide a detailed picture of magma reservoir dynamics at active volcanic systems. Moreover, in successfully reproducing Okmok's 2008 eruption we have also shown the EnKF's potential as a forecasting tool to be used by monitoring agencies. The EnKF technique could theoretically be applied in real time, providing an ongoing, up-to-date model of the magma reservoir and its likelihood of mechanical failure independently of more immediate precursors. Moreover, as a framework the EnKF is very flexible and can easily be adapted for use with different predictive models, as discussed below, and with any data set that could reasonably be predicted by those models. Although this study only uses GPS and InSAR data, other observations such as ground tilt could have also been used if available. Given the relative novelty of this approach in volcanology, however, there are still many questions to ask and technical limitations to overcome before the application of the EnKF can reach its full potential.

First of all, there is the question of how to distinguish changes in source parameters from artifacts of model convergence. Previous synthetic tests of the EnKF predict that the ensemble converges from its initial wide distribution within the first few time steps, with all subsequent changes in the modeled parameters being due primarily to changes in the source (Gregg & Pettijohn, 2016; Zhan & Gregg, 2017). In this study, however, most parameters do not begin to narrow until nearly a year after the start of the assimilation. Although this effect is most likely due to the low magnitudes of deformation during the initial time steps providing the EnKF little basis on which to distinguish the performance of one ensemble member against another, the question of when the results become meaningful still remains. A sudden increase in the modeled overpressure during

2004, for instance, coincides with both the first major period of inflation and the initial convergence of the parameters. Although the observed deformation may be driven by an increase in pressure as modeled, this case is difficult to distinguish from the possibility that the pressure change is an artifact of convergence and that the deformation was driven by changes in other parameters such as the half width.

We must next consider the limitations of the numerical models being used within the EnKF framework. As we develop our workflow we have primarily chosen restrictive models (e.g., axisymmetry and elastic

rheology) that can easily be compared to and benchmarked against accepted analytical solutions (McTigue, 1987; Mogi, 1958; Yang et al., 1988). Although these simplifications make the assimilation computationally easier, actual volcanic systems host a variety of effects that we currently do not account for, including layered, nonelastic, or temperature-dependent rheology (Del Negro et al., 2009; Gregg et al., 2013; Long & Grosfils, 2009; McTigue, 1987), pore pressure (Albino et al., 2018; Grosfils et al., 2015), overlying features such as faults or edifices (Gregg et al., 2018; Grosfils et al., 2015), and far field stresses (Cabaniss et al., 2018; Martí et al., 2016), all of which may alter when and how the reservoir fails. The EnKF, however, is model independent and does not need to be reformulated for each application like other forms of Kalman filters (Evensen, 1994; Grewal & Andrews, 2008; Julier et al., 2000). As our approach is tested and benchmarked, it will be relatively simple to substitute more complex or competing models in order to observe how they may affect the assimilation's outcomes and the resulting conclusions. However, time-dependent models, such as ones that use viscoelasticity or that simulate magma flux directly (Gregg et al., 2018; Le Mével et al., 2016), may be more difficult to incorporate into an EnKF framework. In particular, these formulations pose additional challenges in terms of computational load and in defining the initial conditions. While a time-dependent version of our approach has been tested (Gregg & Pettijohn, 2016), it required running the models from time zero at each time step, which becomes computationally prohibitive.

Although the question of how to define initial conditions is particularly important when using time-dependent models, it should be considered for any implementation of the EnKF. In this study, for instance, the net deformation state of the volcano at the start of our assimilation is not considered due to lack of data. Our models therefore only account for the stresses that built up over the observed period, and any previous stress accumulation may cause tensile and/or Mohr-Coulomb failure to occur sooner than predicted by the assimilation. Ideal targets for future studies would therefore be systems with short recurrence intervals and geodetic observations spanning multiple eruption cycles, such that all observations can be made relative to the end of a previous eruption (e.g., Sierra Negra and Fernandina, Galapagos; Aria/Sakurajima, Japan; and Agung and Sinabung, Indonesia). Regardless, the EnKF is a powerful and flexible tool that could potentially be used to improve our understanding of any system with sufficient data.

Acknowledgments

This work was supported by a U.S. National Science Foundation Graduate Research Fellowship (Albright), grants from the U.S. National Science Foundation (NSF CAREER—1752477, NSF OCE MGG—1634995, Gregg) and U.S. National Aeronautics and Space Administration (80-NSSC19K-0357, Gregg and Lu; and ESI13-0031, Lu and Freymueller). We would like to thank Lei Zhang of Hong Kong Polytechnic University and Jin Woo Kim of Southern Methodist University for the help in acquiring and processing the InSAR data. We are also grateful for helpful discussions with Y. Zhan, C. Pettijohn, H. Cabaniss, R. Goldman, V. Romano, and the UIUC Geodynamics Group. GPS data used in this investigation are available at <https://www.unavco.org/data>. InSAR data were previously published by Lu et al. (2010). Model data in support of this manuscript are published in the PANGAEA data repository and available online (<https://doi.org/10.1594/PANGAEA.904432>).

References

- Albino, F., Amelung, F., & Gregg, P. (2018). The role of pore fluid pressure on the failure of magma reservoirs: Insights from Indonesian and Aleutian arc volcanoes. *Journal of Geophysical Research: Solid Earth*, *123*, 1328–1349. <https://doi.org/10.1002/2017JB014523>
- Allen, J. I., Eknes, M., & Evensen, G. (2003). An ensemble Kalman filter with a complex marine ecosystem model: Hindcasting phytoplankton in the Cretan Sea. *Annales Geophysicae*, *21*(1), 399–411. <https://doi.org/10.5194/angeo-21-399-2003>
- Aoki, Y., Segall, P., Kato, T., Cervelli, P., & Shimada, S. (1999). Imaging magma transport during the 1997 seismic swarm off the Izu Peninsula, Japan. *Science*, *286*(5441), 927–930. <https://doi.org/10.1126/science.286.5441.927>
- Bato, M. G., Pintel, V., & Yan, Y. (2017). Assimilation of deformation data for eruption forecasting: Potentiality assessment based on synthetic cases. *Frontiers in Earth Science*, *5*. <https://doi.org/10.3389/feart.2017.00048>
- Beget, J. E., Larsen, J. F., Neal, C. A., Nye, C. J., & Schaefer, J. R. (2005). Preliminary volcano-hazard assessment for Okmok Volcano, Umnak Island, Alaska (No. RI 2004-3). Alaska Division of Geological & Geophysical Surveys. <https://doi.org/10.14509/7042>
- Biggs, J., Ebmeier, S. K., Aspinall, W. P., Lu, Z., Pritchard, M. E., Sparks, R. S. J., & Mather, T. A. (2014). Global link between deformation and volcanic eruption quantified by satellite imagery. *Nature Communications*, *5*(1). <https://doi.org/10.1038/ncomms4471>
- Biggs, J., Lu, Z., Fournier, T., & Freymueller, J. T. (2010). Magma flux at Okmok Volcano, Alaska, from a joint inversion of continuous GPS, campaign GPS, and interferometric synthetic aperture radar. *Journal of Geophysical Research*, *115*, B12401. <https://doi.org/10.1029/2010JB007577>
- Biggs, J., & Pritchard, M. E. (2017). Global volcano monitoring: What does it mean when volcanoes deform? *Elements*, *13*(1), 17–22. <https://doi.org/10.2113/gselements.13.1.17>
- Brusdal, K., Brankart, J. M., Halberstadt, G., Evensen, G., Brasseur, P., van Leeuwen, P. J., et al. (2003). A demonstration of ensemble-based assimilation methods with a layered OGCM from the perspective of operational ocean forecasting systems. *Journal of Marine Systems*, *40–41*, 253–289. [https://doi.org/10.1016/S0924-7963\(03\)00021-6](https://doi.org/10.1016/S0924-7963(03)00021-6)
- Cabaniss, H. E., Gregg, P. M., & Grosfils, E. B. (2018). The role of tectonic stress in triggering large silicic caldera eruptions. *Geophysical Research Letters*, *45*, 3889–3895. <https://doi.org/10.1029/2018GL077393>
- Del Negro, C., Currenti, G., & Scandura, D. (2009). Temperature-dependent viscoelastic modeling of ground deformation: Application to Etna volcano during the 1993–1997 inflation period. *Physics of the Earth and Planetary Interiors*, *172*(3–4), 299–309. <https://doi.org/10.1016/j.pepi.2008.10.019>
- Evensen, G. (1994). Sequential data assimilation with a nonlinear quasi-geostrophic model using Monte Carlo methods to forecast error statistics. *Journal of Geophysical Research*, *99*(C5), 10,143. <https://doi.org/10.1029/94JC00572>
- Evensen, G. (2003). The Ensemble Kalman Filter: Theoretical formulation and practical implementation. *Ocean Dynamics*, *53*(4), 343–367. <https://doi.org/10.1007/s10236-003-0036-9>
- Evensen, G. (2009a). *Data assimilation: The ensemble Kalman filter* (2nd ed.). Dordrecht, New York: Springer. <https://doi.org/10.1007/978-3-642-03711-5>

- Evensen, G. (2009b). The ensemble Kalman filter for combined state and parameter estimation. *IEEE Control Systems*, 29(3), 83–104. <https://doi.org/10.1109/MCS.2009.932223>
- Fournier, T., Freymueller, J., & Cervelli, P. (2009). Tracking magma volume recovery at Okmok volcano using GPS and an unscented Kalman filter. *Journal of Geophysical Research*, 114, B02405. <https://doi.org/10.1029/2008JB005837>
- Freymueller, J. T., & Kaufman, A. M. (2010). Changes in the magma system during the 2008 eruption of Okmok volcano, Alaska, based on GPS measurements. *Journal of Geophysical Research*, 115, B12415. <https://doi.org/10.1029/2010JB007716>
- Got, J.-L., Carrier, A., Marsan, D., Jouanne, F., Vogfjörð, K., & Villemain, T. (2017). An analysis of the nonlinear magma-edifice coupling at Grímsvötn volcano (Iceland). *Journal of Geophysical Research: Solid Earth*, 122, 826–843. <https://doi.org/10.1002/2016JB012905>
- Gregg, P. M., de Silva, S. L., & Grosfils, E. B. (2013). Thermomechanics of shallow magma chamber pressurization: Implications for the assessment of ground deformation data at active volcanoes. *Earth and Planetary Science Letters*, 384, 100–108. <https://doi.org/10.1016/j.epsl.2013.09.040>
- Gregg, P. M., de Silva, S. L., Grosfils, E. B., & Parmigiani, J. P. (2012). Catastrophic caldera-forming eruptions: Thermomechanics and implications for eruption triggering and maximum caldera dimensions on Earth. *Journal of Volcanology and Geothermal Research*, 241–242(1–12), 1–12. <https://doi.org/10.1016/j.jvolgeores.2012.06.009>
- Gregg, P. M., Le Mével, H., Zhan, Y., Dufek, J., Geist, D., & Chadwick, W. W. (2018). Stress triggering of the 2005 eruption of Sierra Negra Volcano, Galápagos. *Geophysical Research Letters*, 45, 13,288–13,297. <https://doi.org/10.1029/2018GL080393>
- Gregg, P. M., & Pettijohn, J. C. (2016). A multi-data stream assimilation framework for the assessment of volcanic unrest. *Journal of Volcanology and Geothermal Research*, 309, 63–77. <https://doi.org/10.1016/j.jvolgeores.2015.11.008>
- Grewal, M. S., & Andrews, A. P. (2008). *Kalman filtering: Theory and practice using MATLAB* (3rd ed.). Hoboken, NJ: Wiley. <https://doi.org/10.1002/9780470377819>
- Grosfils, E. B. (2007). Magma reservoir failure on the terrestrial planets: Assessing the importance of gravitational loading in simple elastic models. *Journal of Volcanology and Geothermal Research*, 166(2), 47–75. <https://doi.org/10.1016/j.jvolgeores.2007.06.007>
- Grosfils, E. B., McGovern, P. J., Gregg, P. M., Galgana, G. A., Hurwitz, D. M., Long, S. M., & Chestler, S. R. (2015). Elastic models of magma reservoir mechanics: A key tool for investigating planetary volcanism. *Geological Society, London, Special Publications*, 401(1), 239–267. <https://doi.org/10.1144/SP401.2>
- Julier, S., Uhlmann, J., & Durrant-Whyte, H. F. (2000). A new method for the nonlinear transformation of means and covariances in filters and estimators. *IEEE Transactions on Automatic Control*, 45(3), 477–482. <https://doi.org/10.1109/9.847726>
- Larsen, J., Neal, C., Webley, P., Freymueller, J., Haney, M., McNutt, S., et al. (2009). Eruption of Alaska volcano breaks historic pattern. *Eos, Transactions American Geophysical Union*, 90(20), 173. <https://doi.org/10.1029/2009EO200001>
- Larsen, J. F., Śliwiński, M. G., Nye, C., Cameron, C., & Schaefer, J. R. (2013). The 2008 eruption of Okmok Volcano, Alaska: Petrological and geochemical constraints on the subsurface magma plumbing system. *Journal of Volcanology and Geothermal Research*, 264, 85–106. <https://doi.org/10.1016/j.jvolgeores.2013.07.003>
- Le Mével, H., Gregg, P. M., & Feigl, K. L. (2016). Magma injection into a long-lived reservoir to explain geodetically measured uplift: Application to the 2007–2014 unrest episode at Laguna del Maule volcanic field, Chile. *Journal of Geophysical Research: Solid Earth*, 121, 6092–6108. <https://doi.org/10.1002/2016JB013066>
- Long, S. M., & Grosfils, E. B. (2009). Modeling the effect of layered volcanic material on magma reservoir failure and associated deformation, with application to Long Valley caldera, California. *Journal of Volcanology and Geothermal Research*, 186(3–4), 349–360. <https://doi.org/10.1016/j.jvolgeores.2009.05.021>
- Lu, Z., Dzurisin, D., Biggs, J., Wicks, C., & McNutt, S. (2010). Ground surface deformation patterns, magma supply, and magma storage at Okmok volcano, Alaska, from InSAR analysis: 1. Interruption deformation, 1997–2008. *Journal of Geophysical Research*, 115, B00B03. <https://doi.org/10.1029/2009JB006969>
- Lu, Z., Masterlark, T., & Dzurisin, D. (2005). Interferometric synthetic aperture radar study of Okmok volcano, Alaska, 1992–2003: Magma supply dynamics and postemplacement lava flow deformation: INSAR STUDY OF OKMOK VOLCANO. *Journal of Geophysical Research*, 110, B02403. <https://doi.org/10.1029/2004JB003148>
- Mann, D., Freymueller, J., & Lu, Z. (2002). Deformation associated with the 1997 eruption of Okmok volcano, Alaska: DEFORMATION OF OKMOK VOLCANO, ALASKA. *Journal of Geophysical Research*, 107(B4), 2108. <https://doi.org/10.1029/2001JB000163>
- Martí, J., López, C., Bartolini, S., Becerril, L., & Geyer, A. (2016). Stress controls of monogenetic volcanism: A review. *Frontiers in Earth Science*, 4. <https://doi.org/10.3389/feart.2016.00106>
- McGuire, J. J., & Segall, P. (2003). Imaging of aseismic fault slip transients recorded by dense geodetic networks. *Geophysical Journal International*, 155(3), 778–788. <https://doi.org/10.1111/j.1365-246X.2003.02022.x>
- McTigue, D. F. (1987). Elastic stress and deformation near a finite spherical magma body: Resolution of the point source paradox. *Journal of Geophysical Research*, 92(B12), 12931. <https://doi.org/10.1029/JB092iB12p12931>
- Miller, T. P., & Smith, R. L. (1987). Late Quaternary caldera-forming eruptions in the eastern Aleutian arc, Alaska. *Geology*, 15(5), 434–438.
- Miyazaki, S., Segall, P., Fukuda, J., & Kato, T. (2004). Space time distribution of afterslip following the 2003 Tokachi-oki earthquake: Implications for variations in fault zone frictional properties. *Geophysical Research Letters*, 31, L06623. <https://doi.org/10.1029/2003GL019410>
- Mogi, K. (1958). Relations between the eruptions of various volcanoes and the deformations of the ground surfaces around them. *Bulletin of the Earthquake Research Institute*, 36, 99–134.
- Natvik, L.-J., & Evensen, G. (2003). Assimilation of ocean colour data into a biochemical model of the North Atlantic. *Journal of Marine Systems*, 40–41, 127–153. [https://doi.org/10.1016/S0924-7963\(03\)00016-2](https://doi.org/10.1016/S0924-7963(03)00016-2)
- Nooner, S. L., & Chadwick, W. W. (2016). Inflation-predictable behavior and co-eruption deformation at Axial Seamount. *Science*, 354(6318), 1399–1403. <https://doi.org/10.1126/science.aah4666>
- Rubin, A. M. (1995). Propagation of magma-filled cracks. *Annual Review of Earth and Planetary Sciences*, 23(1), 287–336. <https://doi.org/10.1146/annurev.ea.23.050195.001443>
- Segall, P. (2013). Volcano deformation and eruption forecasting. *Geological Society, London, Special Publications*, 380(1), 85–106. <https://doi.org/10.1144/SP380.4>
- Segall, P., & Matthews, M. (1997). Time dependent inversion of geodetic data. *Journal of Geophysical Research*, 102(B10), 22,391–22,409. <https://doi.org/10.1029/97JB01795>
- Seiler, A., Evensen, G., Skjervheim, J.-A., Hove, J., & Vabo, J. G. (2009). Advanced reservoir management workflow using an EnKF based assisted gistory matching method. In *SPE Reservoir Simulation Symposium*. The Woodlands, TX: Society of Petroleum Engineers. <https://doi.org/10.2118/118906-MS>

- Sparks, R. S. J. (2003). Forecasting volcanic eruptions. *Earth and Planetary Science Letters*, *210*(1-2), 1–15. [https://doi.org/10.1016/S0012-821X\(03\)00124-9](https://doi.org/10.1016/S0012-821X(03)00124-9)
- Voight, B., Hoblitt, R. P., Clarke, A. B., Lockhart, A. B., Miller, A. D., Lynch, L., & McMahon, J. (1998). Remarkable cyclic ground deformation monitored in real-time on Montserrat, and its use in eruption forecasting. *Geophysical Research Letters*, *25*(18), 3405–3408. <https://doi.org/10.1029/98GL01160>
- Wilson, G. W., Özkan-Haller, H. T., Holman, R. A., Haller, M. C., Honegger, D. A., & Chickadel, C. C. (2014). Surf zone bathymetry and circulation predictions via data assimilation of remote sensing observations. *Journal of Geophysical Research: Oceans*, *119*, 1993–2016. <https://doi.org/10.1002/2013JC009213>
- Yang, X.-M., Davis, P. M., & Dieterich, J. H. (1988). Deformation from inflation of a dipping finite prolate spheroid in an elastic half-space as a model for volcanic stressing. *Journal of Geophysical Research*, *93*(B5), 4249–4257. <https://doi.org/10.1029/JB093iB05p04249>
- Zhan, Y., & Gregg, P. M. (2017). Data assimilation strategies for volcano geodesy. *Journal of Volcanology and Geothermal Research*, *344*, 13–25. <https://doi.org/10.1016/j.jvolgeores.2017.02.015>